Progress In Electromagnetics Research, Vol. 106, 1–16, 2010

TRANSIENT RESPONSES OF COAXIAL CABLES IN AN ELECTRICALLY LARGE CABIN WITH SLOTS AND WINDOWNS ILLUMINATED BY AN ELECTROMAGNETIC PULSE

J. Wang

Center for Microwave and RF Technologies
Shanghai Jiao Tong University
Shanghai 200240, China

W.-Y. Yin †

Center for Optical and EM Research (COER)
Zhejiang University
Hangzhou 310058, China

J.-P. Fang and Q.-F. Liu

Center for Microwave and RF Technologies
Shanghai Jiao Tong University
Shanghai 200240, China

Abstract—An improved finite-difference time-domain (FDTD) method is proposed for predicting transient responses of coaxial cables which are placed in an electrically large metallic cabin with arbitrary slots and circular windows on its wall. By integrating nodal analysis, multi-conductor transmission line (MTL) equation and FDTD method, we are able to accurately capture electromagnetic interference (EMI) effects on the cables. Our developed algorithm is verified by calculating frequency-dependent transfer impedance of coaxial cables together with induced currents. Numerical calculations are further performed to show the near-end coupled current responses of braided and tubular cables, respectively, and the effects of incident directions and polarizations of the illuminated electromagnetic pulse are both taken into account.

Received 7 June 2010, Accepted 8 July 2010, Scheduled 8 July 2010
Corresponding author: J. Wang (wangjianmath@sjtu.edu.cn).
† Also with Center for Microwave and RF Technologies, Shanghai Jiao Tong University, Shanghai 200240, China.

1. INTRODUCTION

Nowadays, cable-interconnected electronic communication systems are often protected by various metallic cabins or enclosures. Unfortunately, some slots and windows have to be created on their walls for certain purpose. Under such circumstances, they will provide electromagnetic coupling paths and may cause serious electromagnetic interference (EMI) of the inner systems [1]. Therefore, it is very important for us to develop an efficient numerical algorithm for fast characterizing the EMI effect with the overall system structure treated appropriately.

Taking multi-conductor transmission line (MTL) network in a metallic cabin into account in detail, the problem will be very complex due to its multi-scale feature. In the past two decades, several efficient methods have been proposed to handle such a typical EMI problem, such as the method of moments-based iterative technique [2], modified finite-difference time-domain (FDTD) method [3], time-domain integral equation (TD-IE) method [4], and hybrid finite difference/finite volume (FD/FV) method [5], etc. In the implementation of these methods, field-orientated methods are often used to compute the field distribution of the cabin or enclosure. Then, external fields in the vicinity of transmission line network are extracted together with some coupling models [6, 7]. Finally, the voltage and current responses of the transmission line networks can be obtained by solving a set of field-line and even field-circuit coupling equations.

In this paper, we present an improved FDTD method for predicting transient electromagnetic responses of coaxial cables in an electrically large metallic cabin with arbitrary thin slots and circular windows on its wall. Our numerical methodology is mainly based on an effective integration of FDTD method with nodal analysis and multi-conductor transmission line (MTL) equation, which enables us to handle both electrically large metallic cabin with complex geometry and the cables loaded with passive components, and the obliquely incident electromagnetic pulse can take any direction with an arbitrary polarization.

2. PROBLEM DESCRIPTION

Figures 1(a) and (b) show the geometry of a cabin with thin slots around the door, and one rectangular and three circular windows on its wall, respectively. A thin coaxial cable is placed in the cabin, with its parameters shown in Fig. 1(b) and Table 1.

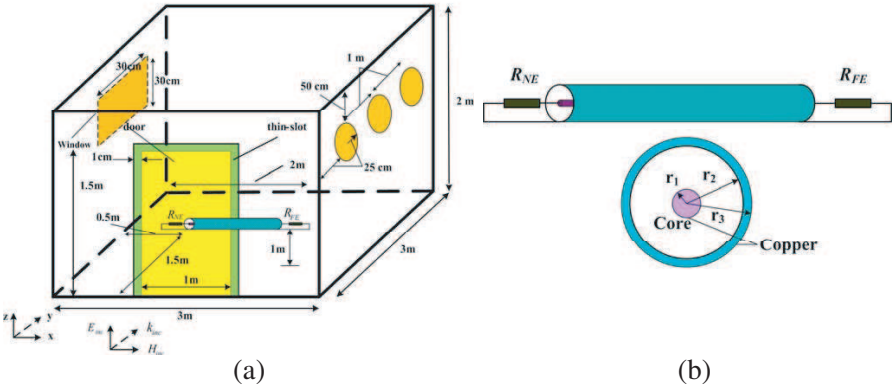

(a) (b)

Figure 1. (a) The geometry of a metallic cabin with thin slots around the door, and one rectangular and three circular windows on its wall, respectively; and (b) the geometry of a coaxial cable placed in the cabin.

Table 1. The parameters of two typical of coaxial cables.

Cable Types	D_0/mm (inner shielding radius)	D_m/mm (outer shielding radius)	r_i/mm (inner core radius)	ε_r (permittivity of insulating layer)
Braided/Tubular Cables	2.95	3.10	0.45	2.3

Table 2. The pulse parameters of three types of EMPs.

Device	Pulse	α/s^{-1}	β/s^{-1}	K
1	Fast-EMP	6.0×10^8	4.0×10^7	1.3
2	Medium-EMP	4.76×10^8	4.0×10^6	1.052
3	Slow-EMP	2.6×10^8	1.5×10^6	1.036

In Fig. 1(a), the incident electromagnetic pulse (EMP) can be described by a double-exponential function as follows [8]:

$$E = E_0 k(e^{-\beta t} - e^{-\alpha t}) \tag{1}$$

where the values of k, α and β are given in Table 2, including fast-, medium-, and slow-EMP, respectively, while the pulse amplitude E_0 can be as high as 50 V/m.

3. METHODOLOGY DESCRIPTION

The cabin structure, shown in Fig. 1(a), has a thin coaxial cable, thin slots around the door, rectangular and circular windows, while the cable is even connected with some passive components. Therefore, a hybrid time-domain method will be proposed for our numerical characterization.

3.1. Modified FDTD Method

3.1.1. Interface Treatment Technique

It is known that in the conformal scheme for modelling perfectly conducting objects [9, 10], three E-field components are updated in the same way as done in the conventional FDTD method. However, the updating equations of the H-field components should be modified on the distorted cells intersected by the PEC boundaries. In the close vicinity of a PEC object, the H-field can be updated according to the Faraday's law as follows:

$$\frac{\partial}{\partial t}\int_S \mathbf{H}\cdot d\mathbf{s} = -\frac{1}{\mu}\oint_L \mathbf{E}\cdot d\mathbf{l}, \tag{2}$$

where S and L denote the area and the boundary of each distorted cell, respectively. The integral path of the E-fields can be detoured along the distorted loop, as shown in Fig. 2(a).

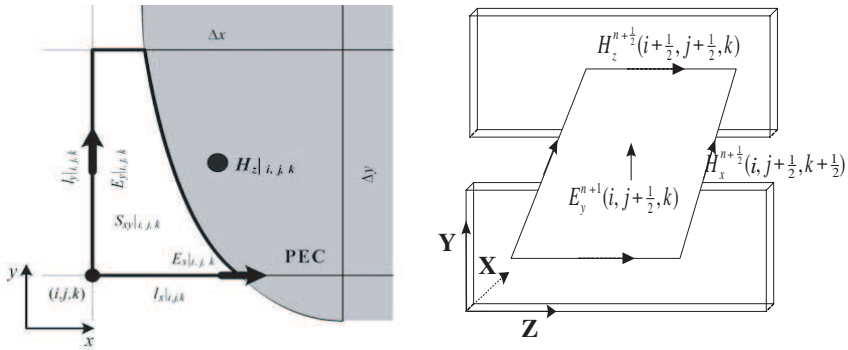

Figure 2. (a) The distorted cells in the conformal FDTD method; and (b) the FDTD mesh for thin slot along the y-axis direction.

In (2), the updating equation of the z-component magnetic field can be rewritten as:

$$H_z\Big|_{i,j,k}^{n+1/2} = H_z\Big|_{i,j,k}^{n-1/2} + \frac{\Delta t}{\mu S_{xy}(i,j,k)} \cdot \left(E_x\Big|_{i,j+1,k}^{n} \cdot l_x|_{i,j+1,k} - E_x\Big|_{i,j,k}^{n} \cdot l_x|_{i,j,k} - E_y\Big|_{i+1,j,k}^{n} \cdot l_y|_{i,j,k} + E_y\Big|_{i+1,j,k}^{n} \cdot l_y|_{i,j,k}\right), \quad (3)$$

where $S_{xy}(i,j,k)$ represents the area of the irregular cell, $l_x|_{i,j,k}$ and $l_y|_{i,j,k}$ are the PEC-free edge lengths along the x- and y-directions, respectively.

3.1.2. Thin-slot Model

In past, the researchers use fine grid to fully discretize the overall metallic enclosure together with thin slots. Under such circumstances, significant increase in memory and running time is required, because very fine time step must be chosen so as to satisfy the Courant-Friedrichs-Lewy (CFL) stability condition. We know that there are three different sub-cellular thin slot algorithms proposed to model thin slots in some metallic enclosures based on the thin slot formalism (TSF), which are denoted by C-TSF, enhanced-TSF, and improved-TSF [11, 12], respectively. With the enhanced-TSF technique, both electric and magnetic field components in the slot, one transverse to the slot, and the other across the slot, can be obtained.

For multiple thin slots along the z-axis direction, as shown in Fig. 2(b), their field updating equations are derived as follows:

$$E_y\Big|_{i,j+1/2,k}^{n+1} = E_y\Big|_{i,j+1/2,k}^{n} + \frac{\Delta t}{\varepsilon_r \varepsilon_0 \Delta z}\left(H_x\Big|_{i,j+1/2,k+1/2}^{n+1/2} - H_x\Big|_{i,j+1/2,k-1/2}^{n+1/2}\right) - \frac{\Delta t}{\varepsilon_r \varepsilon_0 \Delta x}\left(H_z\Big|_{i+1/2,j+1/2,k}^{n+1/2} - H_z\Big|_{i-1/2,j+1/2,k}^{n+1/2}\right), \quad (4)$$

$$H_x\Big|_{i,j+1.2,k+1/2}^{n+1/2} = H_x\Big|_{i,j+1.2,k+1/2}^{n-1/2} + \frac{\Delta t}{\mu_r \mu_0 \Delta z}\left(E_y\Big|_{i+1/2,j,k+1}^{n} - E_y\Big|_{i+1/2,j,k}^{n}\right) - \frac{\Delta t}{\mu_r \mu_0 \Delta y}\left(E_z\Big|_{i,j+1,k+1/2}^{n} - E_z\Big|_{i,j,k+1/2}^{n}\right). \quad (5)$$

3.1.3. Thin-wire Model

In our hybrid FDTD method, we just need to obtain the external fields around the outer layer of the cables used to calculate the induced currents of the outer shield. And the inner currents of the core can be obtained by solving the modified MTL equations. Thus, we just need to deal with the outer layer of the cables when we model these coaxial cables in the cabin.

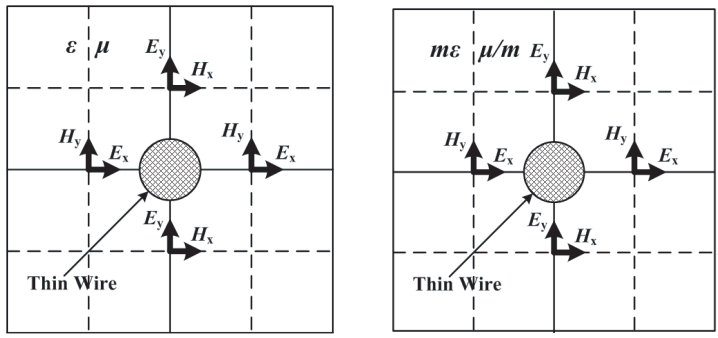

Figure 3. Thin wire and configuration of the adjacent electric and magnetic fields. (a) The original problem; and (b) the modified one.

In order to model the shielded coaxial cable in Fig. 1(b), we can implement thin wire model as proposed in [13] in our simulation. In this method, both adjacent electric and magnetic fields are corrected according to the wire radius, as shown in Figs. 3(a) and (b), respectively. The field correction is carried out by modifying both equivalent permittivity (ε_r) and permeability (μ_r) of the adjacent cells. They are used for calculating the magnetic field components closest to the wire and the closest radial electric field components, respectively, and given by

$$\mu_r' = \mu_r/m, \quad \varepsilon_r' = m\varepsilon_r \tag{6}$$

$$m = \ln(\Delta/a_0)\,/\,\ln(\Delta/a), \quad a_0 = 0.230\Delta, \tag{7}$$

where Δ is the spatial mesh size of the FDTD method, and a_0 is the equivalent radius represented by forcing the tangential components of electric field along the wire axis to be zero.

3.2. Transfer Impedance of the Shielded Cables

In order to predict the transient response of a coaxial cable, the transfer impedance is an important parameter which is directly related to the computation of its distributed voltage sources.

3.2.1. Braided Cable

It is well known that two widely used theoretical models for calculating the transfer impedance of a braided cable at radio frequencies are proposed in [14] and [15], respectively. The Vance's model [14] mainly considers the diffusion of magnetic currents induced in the shield and

the direct leakage of the magnetic field through holes in the braided part at low and high frequencies, respectively. Therefore, its accuracy at lower frequencies is high. While the Tyni's model [15] considers the coupling of fields inside and outside the cable, due to the magnetic flux linkage between the inner and outer braided layers. Therefore, it has high accuracy at high frequencies. We now combine the two models together, and the transfer impedance of the braided cable, as shown in Fig. 4(a), is calculated by

$$Z_T = Z_d + j\omega \left(M_h \pm M_b\right), \tag{8}$$

with

$$Z_d = \frac{4}{\pi d^2 nC\sigma \cos\theta} \cdot \frac{(1+j)\, d/\delta}{\sinh\left((1+j)\, d/\delta\right)}, \tag{9}$$

$$\delta = (\pi f \mu \sigma)^{-1/2} \tag{10}$$

$$M_h = \frac{2\mu_0 C}{\pi \cos\theta} \left(\frac{b}{\pi D_m}\right)^2 \exp\left(-\pi d/b - 2\theta\right), \tag{11}$$

$$M_b = \mp \frac{\mu_0 h}{4\pi D_m} \cdot \left(1 - \tan^2\theta\right), \ and \begin{cases} \theta < \pi/4 \Rightarrow' -' \\ \theta > \pi/4 \Rightarrow' +' \end{cases}, \tag{12}$$

where Z_d is the diffusion impedance, M_b is the per-unit-length braid inductance, M_h is the hole inductance. C is the number of spindles, n is the ends per spindle, d is the diameter over dielectric, σ is the conductivity of the wires, θ is the braid angle, h is the mean distance between the braided spindles, and D_m is the diameter of the over braided cable.

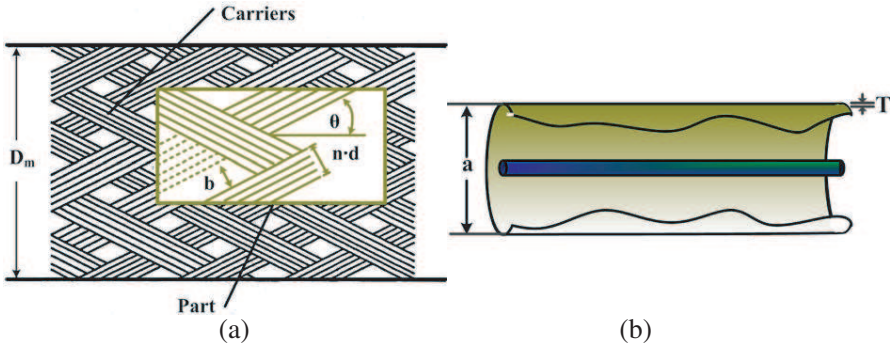

Figure 4. Illustration of two types of shielded cables: (a) braided; and (b) tubular cases.

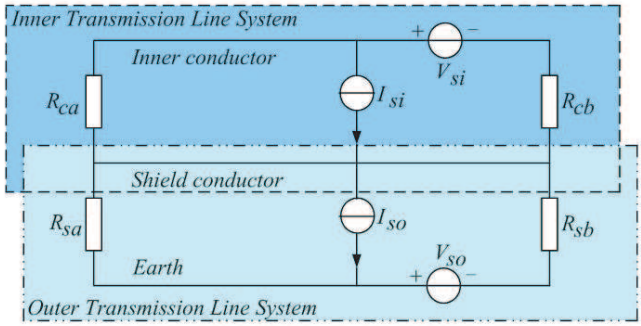

Figure 5. Illustration of the double-MTL model of a shielded cable system.

3.2.2. Tubular Cable

For the tubular cable (as shown in Fig. 4(b)), its transfer impedance is very small. The impedance of the thin tubular cable can be determined by [16]

$$Z_T = \frac{1}{2\pi a\sigma T} \cdot \frac{(1+j)T/\delta}{\sinh((1+j)T/\delta)} \tag{13}$$

where a is its radius, T and σ are the thickness and conductivity of the shielding layer, respectively.

3.3. Field-line EM Coupling Models

As we know, there are two methods to solve the coupling EM problems of shielded cables, i.e., full-wave and effective circuit model methods. If the cable network is complex and its overall structure is electrically large, it is very difficult to handle its EM coupling problems using the full-wave method. One efficient way is that the external fields can be linked with MTL model by introducing a set of distributed voltage and current sources, as proposed in [17] and [18], respectively. In the implementation of the field-line coupling model, the coupling process of electric and magnetic fields can be simply transformed into the coupling of currents and voltages through the transfer impedance between the internal and external shielded cables. As shown in Fig. 5, the shielded cable is described by two transmission line models, i.e., an internal one consisting of the core and the shielding layer of the cable, and an external one consisting of the shielding layer and the reference plane.

The transfer admittance of the cable is very small compared with the transfer impedance, so the transfer admittance is excluded in our model. Thus, one set of MTL equations can be derived by

$$\begin{cases} \frac{\partial}{\partial z}V(z,t) + RI(z,t) + L\frac{\partial}{\partial t}I(z,t) = V_F(z,t) = Z_T(t)^* I_b(z,t) \\ \frac{\partial}{\partial z}I(z,t) + GV(z,t) + C\frac{\partial}{\partial t}V(z,t) = 0 \end{cases} \tag{14}$$

where $V(z,t)$, $I(z,t)$ and $V_F(z,t)$ are the cable voltage, current, and distributed voltage source, respectively; I_b is the induced current of the shielding layer, and Z_T is the transfer impedance. The parameters R, L, G, and C are the per-unit-length resistance, inductance, conductance, and capacitance of the cable, respectively. Using the central-difference scheme, the voltage and current updating equations are obtained by

$$\begin{aligned} \mathbf{I}_k^{n+3/2} = \left(\mathbf{L}\frac{\Delta z}{\Delta t} + \frac{\mathbf{R}}{2}\Delta z\right)^{-1} \Bigg[& \left(\mathbf{L}\frac{\Delta z}{\Delta t} - \frac{\mathbf{R}}{2}\Delta z\right)\mathbf{I}_k^{n+1/2} \\ & -\left(\mathbf{V}_{k+1}^{n+1} - \mathbf{V}_k^{n+1}\right) + \frac{\Delta z}{2}\left(\mathbf{V}_{Fk}^{n+3/2} - \mathbf{V}_{Fk}^{n+1/2}\right)\Bigg], \\ & k = 1, \ldots NDZ; \end{aligned} \tag{15}$$

$$V_k^{n+1} = \left(\mathbf{C}\frac{\Delta z}{\Delta t} + \frac{\mathbf{G}}{2}\Delta z\right)^{-1} \left[\left(\mathbf{C}\frac{\Delta z}{\Delta t} - \frac{\mathbf{G}}{2}\Delta z\right)\mathbf{V}_k^n - \left(\mathbf{I}_k^{n+1/2} - \mathbf{I}_{k-1}^{n+1/2}\right)\right], \quad k = 2, \ldots NDZ. \tag{16}$$

4. NUMERICAL RESULTS AND DISCUSSION

Based on the above mathematical treatment, numerical computations are at first carried out to verify the accuracy of our proposed hybrid FDTD method. Further, the current responses of two types of coaxial cables in a cabin illuminated by an EMP are studied in detail.

4.1. Transfer Impedance of the Shielded Cable

We now calculate the transfer impedance of the URM43 braided cable [19], and Fig. 6 shows the comparison between the calculated and measured results of the transfer impedance magnitude [19]. It is obvious that our improved model has good agreement with the measured transfer impedance over a frequency range ($10^5 \sim 10^8$ Hz). The comparison of the transfer impedances between the braided cable and tubular shielded one is shown in Fig. 6(b). It is seen that, at high frequencies, the transfer impedance of the braided cable increases very fast, while for tubular shielded one, it decreases slowly.

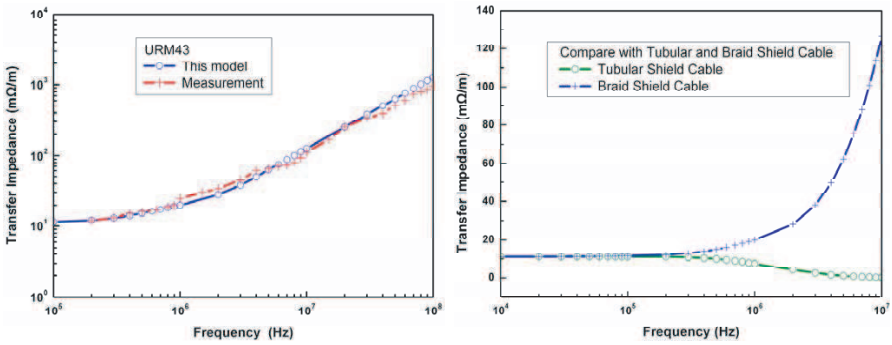

(a) (b)

Figure 6. (a) and (b) comparisons of the transfer impedances obtained by different methods for different cables.

4.2. Induced Currents of a Coaxial Cable above a PEC Plane

Next, we consider the induced currents of a coaxial cable above a PEC ground plane, as shown in Fig. 7(a), which is illuminated by a plane wave. The cable with a length of 2 m is located at 0.1 m away from the ground plane and terminated with two resistors $R_1 = 50\,\Omega$ and $R_2 = 50\,\Omega$ at its near- and far-end, respectively. The inner shielding radius $D_0 = 4.56\,\text{mm}$, outer shielding radius $D_m = 4.99\,\text{mm}$, and the inner core radius $r_i = 1.27\,\text{mm}$. Figs. 7(b) and (c) show the induced currents in comparison with the conventional FDTD method and those presented in [20–22], with good agreements obtained between them. In the theory method, the incident plane wave is expanded in series of cylindrical wave form and the induced currents of the cable shield can be easily obtained by using the EM field boundary conditions on the cable shield surface. Then, we can get the currents of inner conductor by solving the modified TL Equation (14) in frequency form. It can be seen that there is a difference about 0.07 mA between the FDTD methods and the theory method. In fact, the cylindrical wave expansion method is suitable for the long line case and it may introduce some errors in this example which include a cable with finite length of 2 m.

4.3. Current Responses of a Coaxial Cable in a Cabin

As shown in Fig. 1, a coaxial cable loaded with resistors is placed in the cabin. As it is illuminated by an EMP, we use an improved FDTD

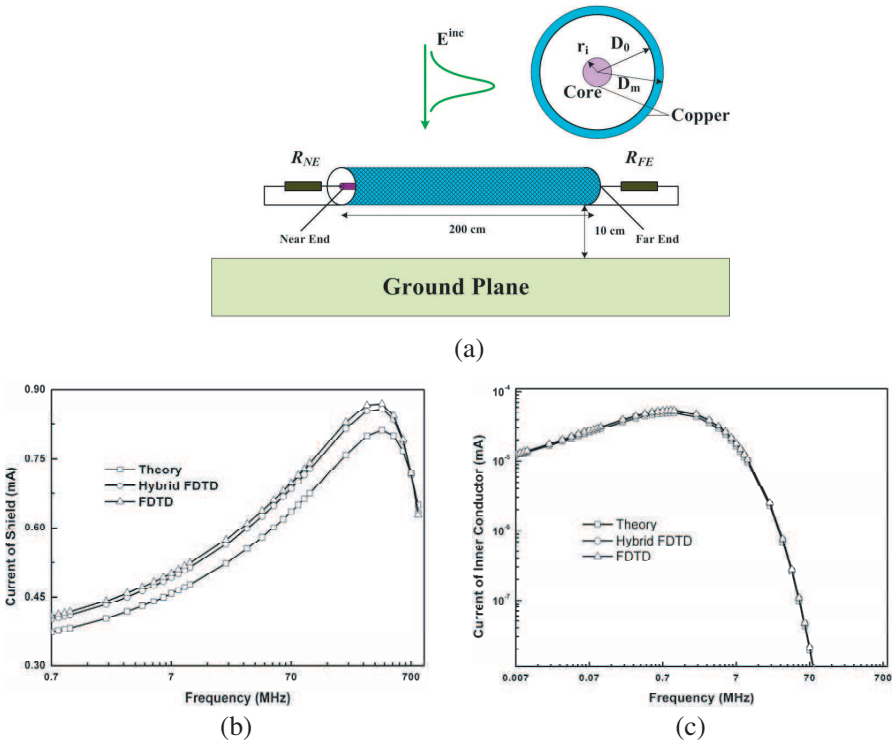

Figure 7. (a) One coaxial cable above a PEC plane; (b) the induced current at the middle point of the shield; and (c) the induced current at the far-end of the inner conductor.

to calculate its current response. In our calculation, the CFL number of our scheme is 0.5, and the cell size is 5 cm. A 10-layered perfectly matched layer (PML) is employed to absorb the outgoing waves. The obliquely incident EMP, as described by a double-exponential function, propagates along the y-direction, with its polarization direction in the z-direction.

Figures 8(a) and (b) show the induced current responses at the near-end of the shield layer and the inner conductor of the braided cable, respectively. Figs. 9(a) and (b) show the current responses of the tubular cable, but with the same geometrical parameters as those in Fig. 8. It is observed that, in comparison with the braided cable, the induced current on the inner core of tubular one is very small (10^{-7} mA), and thus, it has very good performance in shielding effectiveness.

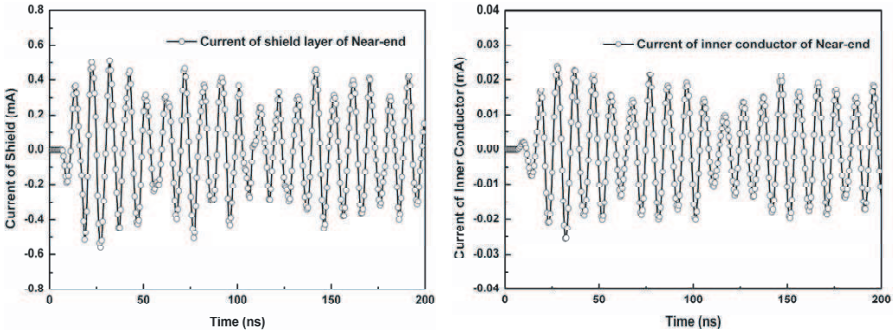

(a) (b)

Figure 8. Near-end induced currents of the braided cable. (a) Currents on the shielding layer; and (b) currents on the inner core.

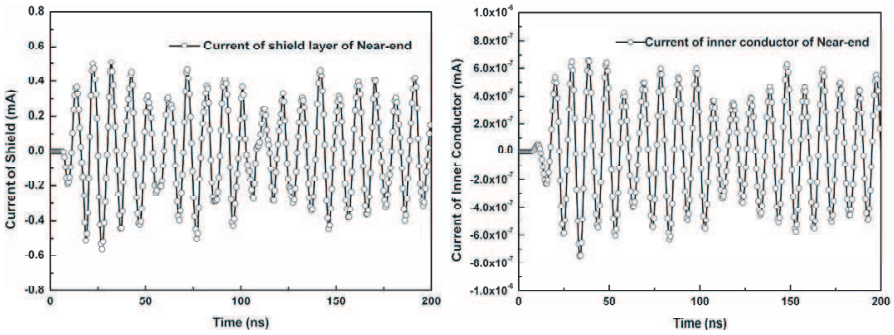

(a) (b)

Figure 9. Near-end induced currents of the tubular cable. (a) Currents on the shielding layer; and (b) currents on the inner core.

Further, Fig. 10 shows the current responses of a braided cable in the cabin illuminated by three types of EMPs, as classified in Table 2, respectively. It is found that more electromagnetic energy can be coupled into the cabin when the cabin is illuminated by a fast EMP, and physically, it includes more high frequency components than that of the other cases, which can easily penetrate into the cabin through the thin slots of the door.

Changing the incident EMP direction, Fig. 11(a) shows the induced currents on the shielding layer of the braided cable in the cabin. It is found that more low frequency energy can be coupled into the cabin through the widows on the left and right panels, when the incident angle $\varphi = 180°$. The coupled energy is the least, if $\varphi = 270°$. Figure 11(b) shows the induced currents on the shielding layer of the

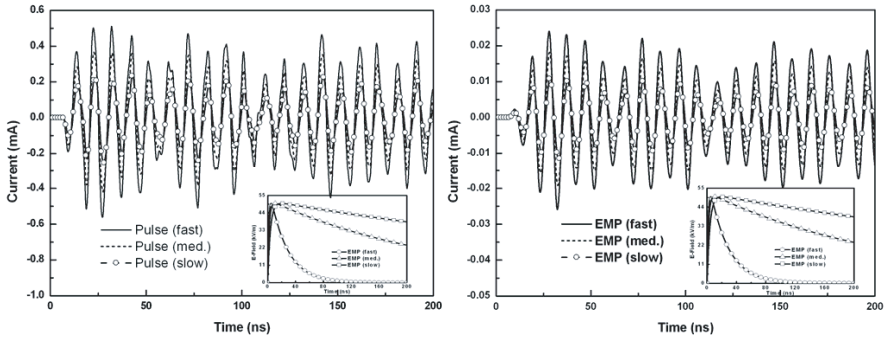

(a) (b)

Figure 10. Near-end coupling currents of a braided cable in the cabin illuminated by three types of pulses. (a) Current on the shielding layer; and (b) current on the inner conductor.

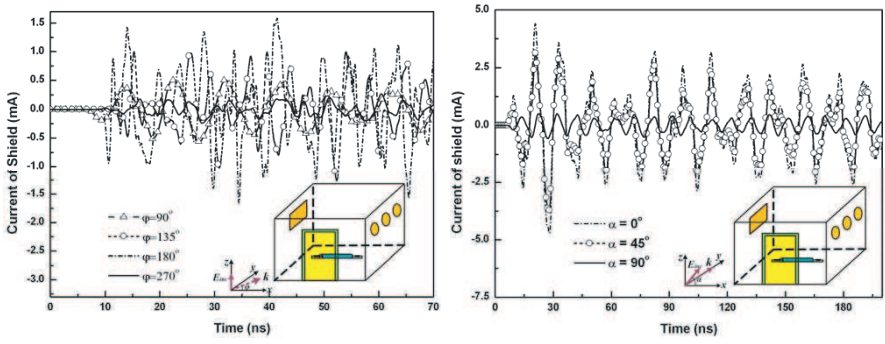

(a) (b)

Figure 11. Near-end coupling currents of a braided cable in the cabin illuminated an EMP with different. (a) Incident directions; and (b) polarizations.

braided cable for different polarizations of the incident EMP. It is found that, when the polarization angle $\alpha = 0°$, the current response is much strong.

Finally, we change the slot width around the door of the cabin from 0.5, 1.0 to 2.0 cm, and the incident EMP is in the same direction as that assumed in Fig. 8. The corresponding current responses of the cables in the cabin are plotted in Figs. 12(a) and (b). It is evident that the induced current responses on the cable are similar for three different slot widths, where the incident wave is a fast-EMP. It can be predicted that, as we further increase the slot width, the induced current magnitudes on the shielding layer and inner conductor of the

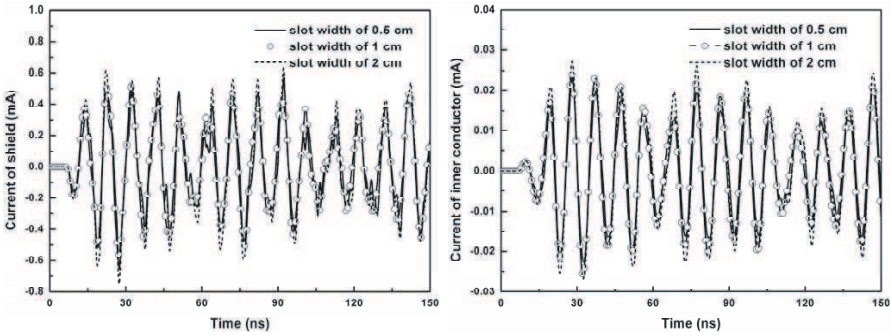

(a) (b)

Figure 12. Near-end coupling currents of the braided cable in the cabin with different slot widths around the door. (a) Currents on the shielding layer; and (b) currents on the inner conductor.

cable will be increased. Obviously, if the energy of the incident pulse is concentrated at high frequency part, these slots will become important coupling paths of the electromagnetic energy.

5. CONCLUSIONS

In this paper, a hybrid time-domain FDTD method is proposed for investigating electromagnetic responses of two types of coaxial cables located in a metallic cabin illuminated by an external EMP, in which nodal analysis, multi-conductor transmission line (MTL) equation are effectively integrated with the FDTD method. Using our developed algorithm, the induced currents in the cables are captured and analyzed, including the incident direction and polarization of the illuminated electromagnetic pulse. Also, the effects of thin slots and circular windows on the cabin wall on the induced current can be characterized accurately. According to the above numerical results, some useful information can be obtained for further electromagnetic protection against unintentional as well as intentional electromagnetic attack on certain platform.

ACKNOWLEDGMENT

The authors appreciate the financial support of the NSF under Grant of 60831002 of China. Wen-Yan Yin also appreciates the financial support from the State Key Lab of MOI, Zhejiang University, Hangzhou of China.

REFERENCES

1. Frei, S., R. G. Jobava, and D. Topchishvili, "Complex approaches for the calculation of EMC problems of large systems," *Proc. IEEE Int. Symp. Electromagn. Compat.*, Vol. 3, 826–831, Aug. 2004.
2. Bayram, Y. and J. L. Volakis, "A generalized MOM-SPICE iterative technique for field coupling to multiconductor tranmission lines in presence of complex structures," *IEEE Trans. Electromagn. Compat.*, Vol. 47, No. 2, 234–246, May 2005.
3. Trakadas, P. T. and C. N. Capsalis, "Validation of a modified FDTD method on non-uniform transmission lines," *Progress In Electromagnetics Research*, Vol. 31, 311–329, 2001.
4. Bagcı, H., A. E. Yılmaz, J. M. Jin, and E. Michielssen, "Fast and rigorous analysis of EMC/EMI phenomena on electrically large and complex cable loaded structure," *IEEE Trans. Electromagn. Compat.*, Vol. 49, No. 2, 361–381, May 2007.
5. Ferrieres, X., J.-P. Paramantier, S. Bertuol, and A. R. Ruddle, "Application of a hybrid finite difference/finite volume method to solve an automotive EMC problem," *IEEE Trans. Electromagn. Compat.*, Vol. 46, No. 4, 624–634, Nov. 2004.
6. Khalaj-Amirhosseini, M., "Analysis of nonuniform transmission lines using the equivalent sources," *Progress In Electromagnetics Research*, Vol. 71, 95–107, 2007.
7. Trakadas, P. T., P. J. Papakanellos, and C. N. Capsalis, "Probabilistic response of a transmission line in a dissipative medium excited by an oblique plane wave," *Progress In Electromagnetics Research*, Vol. 33, 45–68, 2001.
8. Camp, M., H. Gerth, H. Garbe, and H. Haase, "Predicting the breakdown behavior of microcontrollers under EMP/UWB impact using a statistical analysis," *IEEE Trans. Electromagn. Compat.*, Vol. 46, No. 3, 368–379, Aug. 2004.
9. Dey, S. and R. Mittra, "A locally conformal finite-difference time-domain (FDTD) algorithm for modeling three-dimensional perfectly conducting objects," *IEEE Microwave Guided Wave Lett.*, Vol. 7, 273–275, Sep. 1997.
10. Hu, X.-J. and D.-B. Ge, "Study on conformal FDTD for electromagnetic scattering by targets with thin coating," *Progress In Electromagnetics Research*, Vol. 79, 305–319, 2008.
11. Riley, D. J. and C. D. Turner, "Hybrid thin-slot algorithm for the analysis of narrow apertures in finite difference time-domain calculations," *IEEE Trans. Antennas Propagat.*, Vol. 38, No. 12, 1943–1950, Dec. 1990.

12. Liu, Q. F., W. Y. Yin, M. F. Xue, J. F. Mao, and Q. H. Liu, "Shielding characterization of metallic enclosures with multiple slots and a thin-wire antenna loaded: Multiple oblique EMP incidences with arbitrary polarizations," *IEEE Trans. Electromagn. Compat.*, Vol. 51, No. 2, 284–292, May 2009.
13. Noda, T. and S. Yokoyama, "Thin wire representation in finite difference time domain surge simulation," *IEEE Trans. Power Del.*, Vol. 17, No. 3, 840–847, Jul. 2002.
14. Vance, E. F., "Shielding effectiveness of braided wire shields," *IEEE Trans. Electromagn. Compat.*, Vol. EMC-17, No. 2, 71–77, May 1975.
15. Tyni, M., "The transfer impedance of coaxial cables with braided conductors," *Proc. IEEE Electromagn. Compat. Symp.*, 410–418, Wroclaw, Poland, Sep. 1976.
16. Helmers, S. and K. H. Gonschorek, "On the contribution of transfer admittance to external field coupling into shielded cables," *IEEE International Symposium on EMC*, Vol. 1, 2–6, Aug. 1999.
17. Cheldavi, A., D. Ansari, and M. Khalaj-Amirhosseini, "Electromagnetic coupling to circulant symmetric multi-conductor microstrip line," *Progress In Electromagnetics Research*, Vol. 49, 189–201, 2004.
18. Liu, Q. F., W. Y. Yin, M. Tang, P. G. Liu, J. F. Mao, and Q. H. Liu, "Time-domain investigation on cable-induced transient coupling into metallic enclosures," *IEEE Trans. Electromagn. Compat.*, Vol. 51, No. 4, 953–962, Nov. 2002.
19. Sali, S., "An improved model for the transfer impedance calculations of braided coaxial cables," *IEEE Trans. Electromag. Compat.*, Vol. 33, No. 2, 139–143, May 1991.
20. Bates, C. P. and G. T. Hawley, "A model for currents and voltages Induced within long Transmission cables by an electromagnetic wave," *IEEE Trans. Electromagn. Compat.*, Vol. 13, No. 4, 18–31, Nov. 1971.
21. Xie, H., J. Wang, R. Fan, and Y. Liu, "Study of loss effect of transmission lines and validity of a spice model in electromagnetic topology," *Progress In Electromagnetics Research*, Vol. 90, 89–103, 2009.
22. Chedid, M., I. Belov, and P. Leisner, "Electromagnetic coupling to a wearable application based on coaxial cable architecture," *Progress In Electromagnetics Research*, Vol. 56, 109–128, 2006.